Stabilized Shock Hydrodynamics: III.
A New Stabilization Concept for Lagrangian Computations☆

G. Scovazzi[a,*]

[a] *1431 Computational Shock- and Multi-physics Department, Sandia National Laboratories, P.O. Box 5800, MS 1319, Albuquerque, NM 87185-1319, USA*

Abstract

A new stabilized method based on a continuous, piece-wise linear approximation of the equations for Lagrangian shock hydrodynamics is presented. Numerical instabilities are controlled by a stabilizing operator derived using the variational multiscale analysis paradigm. The proposed approach satisfies global conservation and Galilean invariance properties, and hinges upon the interpretation of the Lagrangian shock hydrodynamics equations as a nonlinear system of wave propagation equations.

Key words: Lagrangian shock hydrodynamics, stabilized methods, variational multiscale analysis, updated Lagrangian formulation, hourglass control, nodal finite element method.

1. Introduction

In recent years, renewed effort has been devoted to the technical advancement of Lagrangian shock hydrodynamics algorithms (*hydrocodes* in short), spurred by the current and foreseeable computational challenges in terms of physical and geometric complexity (for a non-exhaustive list of publications on this topic, see [1, 2, 4, 5, 8–12, 15, 16, 32–38, 44–46]). In particular, the developments in [2, 8–12, 36–38] focussed on improving the robustness of simulations with respect to mesh distortion, while maintaining second-order accuracy in smooth regions of the flow.

This article presents a new stabilization concept in which the variational multiscale approach [20, 21, 27] is applied to Lagrangian shock hydrodynamic flows in combination with piece-wise linear, continuous finite element approximations. Specifically, the proposed method adopts a continuous piece-wise linear approximation of both thermodynamic and kinematic variables, contrary to more traditional approaches in shock hydrodynamics, which rely on a piece-wise constant discretization of the thermodynamic variables. A multiscale decomposition of the solution into coarse (discretely representable) scales and fine (subgrid) scales is adopted. An approximation of the subgrid-scale component of the solution is used to control instabilities of acoustic type, which are typically responsible for spurious hourglass modes in the case of quadrilateral/hexahedral elements, or pressure instabilities (often referred to as element artificial stiffness) in the case of triangular/tetrahedral elements (see [3, 19] for a detailed introduction to the subject). The solution enrichment by fine-scale subgrid contributions provides enhanced stability without reducing accuracy, as the method relies on residual-based (therefore variationally consistent) approximations of the fine scales (see also [47]). Stabilization operators are developed in the context of smooth flows, and need to be complemented by appropriate discontinuity capturing operators (e.g., artificial viscosities [53]), whenever shock wave discontinuities are expected.

The present work stems from earlier work [43, 44], and represents a considerable advance from many points of view. The method leverages a variational formulation of the shock hydrodynamics equations in updated Lagrangian form, for which most integrals are computed directly in the current configuration (see [3] for details on this nomenclature). This strategy contrasts with the formulation in [44], which was posed in the original configuration (total or pure Lagrangian approach [3]). The proposed updated Lagrangian approach allows for a reduction in the computational costs, as the deformation gradient mapping from the original to the current configuration does not need to be evaluated explicitly, but is implicitly calculated by updating the coordinates of the mesh nodes. In addition, algorithms for fast dynamics posed in the current configuration usually enjoy improved discrete invariance and objectivity properties relative to corresponding algorithms cast in the original configuration. This is due to the fact that the discretization of the unsymmetric Piola stress tensor does not always preserve the same invariance properties of the analytical counterpart (see [3, 19, 49] and references therein, for more details).

The rest of the exposition is organized as follows: Section 2 is devoted to presenting the equations of Lagrangian hydrodynamics and highlighting their structure as a nonlinear (mixed) system for acoustic wave propagation. In Section 3, the variational multiscale analysis is applied to a simplified linear problem, to make the reader familiar with the fundamental stabi-

☆This research was partially funded by the DOE NNSA Advanced Scientific Computing Program and the Computer Science Research Institute at Sandia National Laboratories. Sandia is a multiprogram laboratory operated by Sandia Corporation, a Lockheed Martin Company, for the United States Department of Energy under contract DEAC04-94-AL85000.

*Corresponding author

Email addresses: gscovaz@sandia.gov (G. Scovazzi)

lization concepts in a simpler setting. In Section 4, the general variational multiscale stabilization framework for the fully nonlinear case is proposed. Section 5 investigates the Galilean invariance and conservation properties of the proposed formulation, while conclusions are summarized in Section 6. For extensive numerical computations, the reader should refer to [48], in which the general approach described here is applied in combination with a second-order predictor/multi-corrector time integrator. A complete von Neumann stability and accuracy analysis of this time integrator is presented in [47], for the linearized, one-dimensional Lagrangian hydrodynamics equations.

2. Equations of Lagrangian shock hydrodynamics

The classical equations of Lagrangian shock hydrodynamics govern the rate of change in position, momentum and energy of a compressible body of fluid, as it deforms. Let Ω_0 and Ω be open sets in $\mathbb{R}^{n_d}$ (where n_d is the number of spatial dimensions). The *deformation*

$$\boldsymbol{\varphi} : \Omega_0 \to \Omega = \boldsymbol{\varphi}(\Omega_0) \ , \tag{1}$$

$$\boldsymbol{X} \mapsto \boldsymbol{x} = \boldsymbol{\varphi}(\boldsymbol{X}, t) \ , \quad \forall \boldsymbol{X} \in \Omega_0, \ t \geq 0 \ , \tag{2}$$

maps the material coordinate $\boldsymbol{X}$, representing the initial position of an infinitesimal material particle of the body, to $\boldsymbol{x}$, the position of that particle in the current configuration (see Fig. 1). Ω_0 is the domain occupied by the body in its initial configuration, with boundary $\partial\Omega_0$. $\boldsymbol{\varphi}$ maps Ω_0 to Ω, the domain occupied by the body in its current configuration, with boundary $\partial\Omega$. $\boldsymbol{\varphi}$ is usually a *smooth*, invertible map, so that the *deformation gradient*, and the *deformation Jacobian determinant* can be defined as

$$\boldsymbol{F} = \nabla_x \boldsymbol{\varphi} \ , \quad \text{or, in index notation,} \quad F_{iA} = \frac{\partial \varphi_i}{\partial X_A} = \frac{\partial x_i}{\partial X_A} \ , \tag{3}$$

$$J = \det(\boldsymbol{F}) \ , \tag{4}$$

where ∇_x is the gradient in the original configuration. In the domain Ω, the equations for the displacement update and conservation of mass, momentum, and energy read:

$$\dot{\boldsymbol{u}} = \boldsymbol{v} \ , \tag{5}$$

$$\rho J = \rho_0 \ , \tag{6}$$

$$\rho \dot{\boldsymbol{v}} = \rho \, \boldsymbol{b} + \nabla_x \cdot \boldsymbol{\sigma} \ , \tag{7}$$

$$\rho \dot{\epsilon} = \rho \, r + \nabla_x \boldsymbol{v} : \boldsymbol{\sigma} + \nabla_x \cdot \boldsymbol{q} \ . \tag{8}$$

Here, ∇_x and $\nabla_x \cdot$ are the current configuration gradient and divergence operators, and $\dot{(\cdot)}$ indicates the material, or Lagrangian, time derivative. $\boldsymbol{u} = \boldsymbol{x} - \boldsymbol{X}$ is the displacement vector, ρ_0 is the reference (initial) density, ρ is the (current) density, $\boldsymbol{v}$ is the velocity, $\boldsymbol{b}$ is the body force (e.g., gravity), $\boldsymbol{\sigma}$ is the symmetric Cauchy stress tensor, r is the energy source term, and $\boldsymbol{q}$ is the heat flux. Using index notation, $\boldsymbol{\sigma}^T : \nabla_x \boldsymbol{v} = \sigma_{ji} \, \partial_{x_i} v_j$, and $\nabla_x \boldsymbol{v} : \boldsymbol{\sigma} = \boldsymbol{\sigma} : \nabla_x \boldsymbol{v} = \boldsymbol{\sigma}^T : \nabla_x \boldsymbol{v}$, since $\boldsymbol{\sigma}$ is symmetric. We also denote by $E = \epsilon + \boldsymbol{v} \cdot \boldsymbol{v}/2$ the total energy, the sum of the internal energy ϵ and the kinetic energy $\boldsymbol{v} \cdot \boldsymbol{v}/2$. E, ϵ, $\boldsymbol{b}$, r are measured per unit mass.

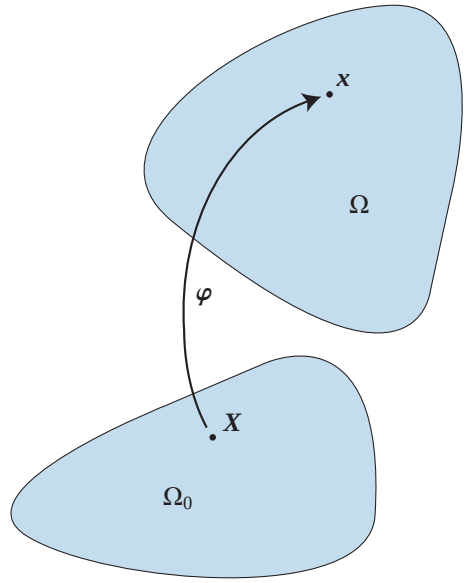

Figure 1: Sketch of the Lagrangian map $\boldsymbol{\varphi}$.

Remark1. Equations (5)–(8) are most commonly adopted in shock-hydrodynamics algorithms [5], and make use of the quasi-linear rather than the conservative form of the internal energy equation. The sum of the internal energy equation (8) and the kinetic energy equation (the product of (7) by the velocity vector $\boldsymbol{v}$) yields the equation for the conservation of total energy.

Remark2. Although (8) is not in conservative form, it can still be used to develop a globally conservative variational formulation, as shown in Section 5.2 in the general case, and [48] for a specific predictor/multi-corrector time integrator.

Assuming that the boundary $\partial\Omega$ is partitioned as $\partial\Omega = \partial\Omega^g \cup \partial\Omega^h$, $\partial\Omega^g \cap \partial\Omega^h = \emptyset$, *displacement boundary conditions* are enforced on the *Dirichlet* boundary $\partial\Omega^g$, that is,

$$\boldsymbol{u}|_{\partial\Omega^g} = \boldsymbol{u}_{bc}(\boldsymbol{x}, t) \ , \tag{9}$$

and *traction boundary conditions* are enforced on the *Neumann* boundary $\partial\Omega^h$, by means of a physical traction vector $\boldsymbol{t}$, that is,

$$\boldsymbol{\sigma}\boldsymbol{n}|_{\partial\Omega^h} = \boldsymbol{t}(\boldsymbol{x}, t) \ . \tag{10}$$

Equations (5)–(8), and boundary conditions (9)-(10) completely define the evolution of the system, once constitutive relationships for the stress $\boldsymbol{\sigma}$ and heat flux $\boldsymbol{q}$ are specified, together with appropriate initial conditions.

2.1. Constitutive laws

The analysis presented in what follows is specific to materials with no deformation strength. In this case, the Cauchy stress $\boldsymbol{\sigma}$ reduces to an isotropic tensor, dependent only on the thermodynamic pressure:

$$\boldsymbol{\sigma} = -p \boldsymbol{I}_{n_d \times n_d} \ , \tag{11}$$

An equation of state of the type

$$p = \hat{p}(\rho, \epsilon) \ , \tag{12}$$

is assumed. For example, equations of state of Mie-Grüneisen type are compatible with (12), namely

$$\hat{p}(\rho, \epsilon) \ = \ f_1(\rho) + f_2(\rho)\epsilon \ , \tag{13}$$

and apply to materials such as compressible ideal gases, co-volume gases, high explosives, etc. (See [39] for more details.) Ideal gases satisfy (13), with $f_1 = 0$ and $f_2 = (\gamma - 1)\rho$, to yield

$$\hat{p}(\rho, \epsilon) = (\gamma - 1)\rho\epsilon \ . \tag{14}$$

2.2. Structure of the Lagrangian shock hydrodynamics flows

It is important at this point to further elaborate on the structure of the Lagrangian shock hydrodynamic equations, because of the important implications on the choice of stabililzation techniques for the discrete variational formulation. To this end, recall that, in general, if an equation of state of the type $\epsilon = \hat{\epsilon}(\rho, p)$ exists, then

$$d\epsilon = \left.\frac{\partial \epsilon}{\partial \rho}\right|_p d\rho + \left.\frac{\partial \epsilon}{\partial p}\right|_\rho dp \ . \tag{15}$$

Assuming, without loss of generality, $\boldsymbol{q} = \boldsymbol{0}$ and $r = 0$, equation (15) can be used together with the mass conservation equation in differential form

$$\dot{\rho} + \rho \nabla_x \cdot \boldsymbol{v} = 0 \ , \tag{16}$$

to rearrange the energy equation (8):

$$\begin{aligned} 0 &= \rho\dot{\epsilon} + p\nabla_x \cdot \boldsymbol{v} \\ &= \rho \left.\frac{\partial \epsilon}{\partial \rho}\right|_p \dot{\rho} + \rho \left.\frac{\partial \epsilon}{\partial p}\right|_\rho \dot{p} + p\nabla_x \cdot \boldsymbol{v} \\ &= \rho \left.\frac{\partial \epsilon}{\partial p}\right|_\rho \left(\dot{p} + \frac{\frac{p}{\rho} - \rho \left.\frac{\partial \epsilon}{\partial \rho}\right|_p}{\left.\frac{\partial \epsilon}{\partial p}\right|_\rho} \nabla_x \cdot \boldsymbol{v} \right) \ , \end{aligned} \tag{17}$$

where, for a general compressible flow, $\rho \left.\partial_p \epsilon\right|_\rho \neq 0$. It is possible to further manipulate the previous result using thermodynamic identities. First note that, by standard calculus derivations,

$$\left(\left.\frac{\partial \epsilon}{\partial p}\right|_\rho \right)^{-1} = \left.\frac{\partial p}{\partial \epsilon}\right|_\rho \ . \tag{18}$$

By the Gibbs identity (i.e., the combined first and second law of thermodynamics) $d\epsilon - p/\rho^2 d\rho = \theta d\eta$ (θ being the temperature and η the entropy per unit mass),

$$\frac{p}{\rho} = \rho \left.\frac{\partial \epsilon}{\partial \rho}\right|_\eta \ . \tag{19}$$

Combining (18) and (19) in the term multiplying the divergence in (17) yields

$$\begin{aligned} \frac{\frac{p}{\rho} - \rho \left.\frac{\partial \epsilon}{\partial \rho}\right|_p}{\left.\frac{\partial \epsilon}{\partial p}\right|_\rho} &= \rho \left.\frac{\partial p}{\partial \epsilon}\right|_\rho \left(\left.\frac{\partial \epsilon}{\partial \rho}\right|_\eta - \left.\frac{\partial \epsilon}{\partial \rho}\right|_p \right) \\ &= \rho \left(\left.\frac{\partial p}{\partial \epsilon}\right|_\rho \left.\frac{\partial \epsilon}{\partial \rho}\right|_\eta - \left.\frac{\partial p}{\partial \epsilon}\right|_\rho \left.\frac{\partial \epsilon}{\partial \rho}\right|_p \right) \end{aligned} \tag{20}$$

Equation (20) can be further simplified recalling that a thermodynamic relation of the type $p = \hat{p}(\rho, \epsilon)$ yields

$$dp = \left.\frac{\partial p}{\partial \rho}\right|_\epsilon d\rho + \left.\frac{\partial p}{\partial \epsilon}\right|_\rho d\epsilon \ , \tag{21}$$

and, particularly,

$$0 = \left.\frac{\partial p}{\partial \rho}\right|_p = \left.\frac{\partial p}{\partial \rho}\right|_\epsilon + \left.\frac{\partial p}{\partial \epsilon}\right|_\rho \left.\frac{\partial \epsilon}{\partial \rho}\right|_p \ . \tag{22}$$

Substituting (22) into (20) yields

$$\begin{aligned} \frac{\frac{p}{\rho} - \rho \left.\frac{\partial \epsilon}{\partial \rho}\right|_p}{\left.\frac{\partial \epsilon}{\partial p}\right|_\rho} &= \rho \left(\left.\frac{\partial p}{\partial \epsilon}\right|_\rho \left.\frac{\partial \epsilon}{\partial \rho}\right|_\eta - \left.\frac{\partial p}{\partial \epsilon}\right|_\rho \left.\frac{\partial \epsilon}{\partial \rho}\right|_p \right) \\ &= \rho \left(\left.\frac{\partial p}{\partial \epsilon}\right|_\rho \left.\frac{\partial \epsilon}{\partial \rho}\right|_\eta + \left.\frac{\partial p}{\partial \rho}\right|_\epsilon \right) \\ &= \rho \left.\frac{\partial p}{\partial \rho}\right|_\eta \\ &= \rho c_s^2 \ , \end{aligned} \tag{23}$$

where c_s is the isentropic speed of sound in the medium. Hence (17) reduces to

$$0 = \rho \left.\frac{\partial \epsilon}{\partial p}\right|_\rho \left(\dot{p} + \rho c_s^2 \nabla_x \cdot \boldsymbol{v} \right) \ . \tag{24}$$

The term $\rho \left.\partial_p \epsilon\right|_\rho \neq 0$ can be simplified in (24), and the momentum and energy equations can be combined into the mixed, first-order system form of a nonlinear wave equation in $\boldsymbol{v}$ and p:

$$0 = \rho\dot{\boldsymbol{v}} + \nabla_x p \ , \tag{25}$$

$$0 = \dot{p} + \rho c_s^2 \nabla_x \cdot \boldsymbol{v} \ . \tag{26}$$

Remark3. It is important to recognize the relation between $\left.\partial_p \epsilon\right|_\rho$ and the Grüneisen parameter Γ, defined as

$$\Gamma = \frac{1}{\rho \left.\frac{\partial \epsilon}{\partial p}\right|_\rho} = \frac{1}{\rho} \left.\frac{\partial p}{\partial \epsilon}\right|_\rho \ . \tag{27}$$

The product $\rho\ \Gamma$ varies only mildly with as a function of the thermodynamic state of a fluid system, as long as the state itself is far from phase transition [39]. In the case of an ideal gas satisfying a γ-law equation of state, it is easy to derive $\rho\ \Gamma = \gamma - 1 =$ constant.

Remark4. The structure of (25)–(26) can be best appreciated in a simplified case, when the small strain approximation is applied (i.e., $\nabla_x \approx \nabla_X$), and time and space variations of density and speed of sound are neglected (see also [43]). In this case, the sum of the divergence of the momentum equation and the time derivative of the energy equation yields

$$0 = \ddot{p} - c_s^2 \Delta_X p \ , \tag{28}$$

where $\Delta_X(\cdot) = \nabla_X \cdot (\nabla_X(\cdot))$ is the Laplace operator. Taking instead the sum of the time derivative of the momentum equation and the gradient of the energy equation,

$$\mathbf{0} = \ddot{\boldsymbol{v}} - c_s^2 \Delta_X \boldsymbol{v} \ . \tag{29}$$

Therefore, the pressure and each of the velocity components abide a wave equation, with speed of propagation of disturbances given by c_s.

3. Variational multiscale analysis of the linearized problem

Consider the linearized case, as a first attempt in developing a stabilized formulation. Interestingly, the work that led to the present article was first developed in the general nonlinear setting and only later restricted to the simpler linear case. However, with the purpose of most clearly discussing the main ideas, the linearized case is introduced first. Recalling that in the small strain approximation the mesh is considered fixed, the discussion can be limited to the momentum equation (7) and energy equation (8), since the mass and displacement updates reduce to trivial statements. As a point of note, it will be clear from what follows that the variational multiscale analysis assumes that fine scales are small with respect to the coarse scales, in some integral sense. As a consequence, this approach applies naturally to smooth flow fields, and is less appropriate in the presence of solution discontinuities. This point is of particular importance in the nonlinear case, for which variational multiscale operators are based on a *locally* linearized approach.

3.1. Variational equations

Neglecting body forces, heat fluxes, and heat sources, and assuming, without loss of generality, homogeneous Dirichlet boundary conditions for the velocity, the variational statement of (25)–(26), can be expressed as:

Find $p \in \mathcal{S}_\gamma$, $\boldsymbol{v} \in \mathcal{S}_\kappa$, such that, $\forall \psi \in \mathcal{V}_\gamma$, $\forall \boldsymbol{\psi} \in \mathcal{V}_\kappa$,

$$0 = \int_\Omega \boldsymbol{\psi} \cdot (\rho \dot{\boldsymbol{v}}) \ \mathrm{d}\Omega - \int_\Omega \nabla_x \cdot \boldsymbol{\psi} \ p \, \mathrm{d}\Omega \ , \tag{30}$$

$$0 = \int_\Omega \psi \left(\dot{p} + \rho c_s^2 \ \nabla_x \cdot \boldsymbol{v} \right) \mathrm{d}\Omega \ , \tag{31}$$

where $\nabla_x = \nabla_X$, $\Omega = \Omega_0$, and ρ and c_s are assumed constant. In particular, $\mathcal{S}_\kappa$ denotes the *trial* space of admissible values for the kinematic variables (velocities, in this case, with boundary conditions strongly embedded in the function space definition), and $\mathcal{S}_\gamma$ the trial space of admissible thermodynamic states (pressures). In addition, *test* spaces have been introduced: $\mathcal{V}_\kappa$ is the space of variations for the kinematic variables (compatible with the boundary conditions), and $\mathcal{V}_\gamma$ is the space of variations for the thermodynamic variables.

3.2. Variational multiscale analysis and stabilization

The variational multiscale analysis of (30)–(31) is accomplished by decomposing the exact solution state vector $\boldsymbol{Y} = [\boldsymbol{v}^T, p]^T \in \mathcal{S}$ as $\boldsymbol{Y} = \boldsymbol{Y}^h + \boldsymbol{Y}'$. $\boldsymbol{Y}^h \in \mathcal{S}^h$ is the *mesh*- or *coarse*-scale solution, belonging to the discrete approximation space $\mathcal{S}^h$. $\boldsymbol{Y}' \in \mathcal{S}'$ is the *subgrid*- or *fine*-scale solution, the component of the solution not represented on the computational mesh. In view of the adopted boundary conditions, the following choice of function spaces can be made

$$\mathcal{S}_\kappa^h = \mathcal{V}_\kappa^h = \Big\{ \boldsymbol{\psi}^h \in (C^0(\Omega))^{n_d} : \boldsymbol{\psi}^h\big|_{\Omega_e} \in (\mathcal{P}_1(\Omega_e))^{n_d}, \quad \boldsymbol{\psi}^h = \mathbf{0} \text{ on } \partial\Omega^g = \partial\Omega \Big\} \ , \tag{32}$$

$$\mathcal{S}_\gamma^h = \mathcal{V}_\gamma^h = \Big\{ \psi^h \in C^0(\Omega) : \psi^h\big|_{\Omega_e} \in \mathcal{P}_1(\Omega_e), \Big\} \ , \tag{33}$$

where $\mathcal{P}_1(\Omega_e)$ is the space of piece-wise linear polynomials over the element e, n_d is the number of space dimensions, and homogeneous Dirichlet boundary conditions have been incorporated (strongly) into the definition of the function spaces. Hence, $\mathcal{S} = \mathcal{S}^h \bigoplus \mathcal{S}'$ (here $\bigoplus$ does not denote an orthogonal sum decomposition), and analogously, $\mathcal{V} = \mathcal{V}^h \bigoplus \mathcal{V}'$. We obtain

$$\boldsymbol{v} = \boldsymbol{v}^h + \boldsymbol{v}' \ , \tag{34}$$

$$p = p^h + p' \ , \tag{35}$$

so that (30)–(31), when tested on $\mathcal{V}_\kappa^h$ and $\mathcal{V}_\gamma^h$, respectively, reduce to

$$\int_\Omega \boldsymbol{\psi}^h \cdot \rho(\dot{\boldsymbol{v}}^h + \dot{\boldsymbol{v}}') \, \mathrm{d}\Omega - \int_\Omega (\nabla_x \cdot \boldsymbol{\psi}^h)(p^h + p') \, \mathrm{d}\Omega = 0 \ , \tag{36}$$

$$\int_\Omega \psi^h \left(\dot{p}^h + \dot{p}' + \rho \, c_s^2 (\nabla_x \cdot (\boldsymbol{v}^h + \boldsymbol{v}') \right) \mathrm{d}\Omega = 0 \ . \tag{37}$$

Equation (37) can be rearranged, using integration by parts, as follows:

$$\int_\Omega \psi^h \left(\dot{p}^h + \dot{p}' + \rho \, c_s^2 \, (\nabla_x \cdot \boldsymbol{v}^h) \right) \mathrm{d}\Omega - \int_\Omega \nabla_x \psi^h \ \cdot \left(\rho \, c_s^2 \, \boldsymbol{v}' \right) \mathrm{d}\Omega + \sum_{e=1}^{n_{el}} \int_{\partial\Omega_e} \psi^h \left(\rho \, c_s^2 \, \boldsymbol{v}' \right) \cdot \boldsymbol{n}_e \ \mathrm{d}(\partial\Omega_e) = 0 \ , \tag{38}$$

where $\boldsymbol{n}_e$ indicates the outward pointing normal with respect to the element e. Recalling now that ψ^h is continuous across the interface between elements, and that ρ and c_s are constant in the linearized case, one can express the last term in (38) using the following identity, often employed in discontinuous Galerkin formulations:

$$\sum_{e=1}^{n_{el}} \int_{\partial\Omega_e} \psi^h \left(\rho \, c_s^2 \, \boldsymbol{v}' \right) \cdot \boldsymbol{n}_e \ \mathrm{d}(\partial\Omega_e) = \int_{\partial\Omega} \psi^h \left(\rho \, c_s^2 \, \boldsymbol{v}' \right) \cdot \boldsymbol{n} \ \mathrm{d}(\partial\Omega) + \int_{\tilde{\mathcal{E}}} \psi^h \, \rho \, c_s^2 \ [\![\boldsymbol{v}']\!] \ \mathrm{d}\tilde{\mathcal{E}} \ . \tag{39}$$

The term $[\![\boldsymbol{w}]\!] = \boldsymbol{w}^- \cdot \boldsymbol{n}^- + \boldsymbol{w}^+ \cdot \boldsymbol{n}^+$ is often referred to as the jump operator, with the superscripts $^\pm$ indicating the values of $\boldsymbol{w}$ and $\boldsymbol{n}$ on either side of an interface between two elements (i.e., an edge or face in the interior of the domain). $\tilde{\mathcal{E}}$ denotes the set of interior element interfaces. Note that *no approximation* has been made so far (the fields $\boldsymbol{v}^h$, $\boldsymbol{v}'$, p^h, p' are assumed to be known *exactly*). In order to obtain a viable stabilization strategy, a few conditions on the terms in the coarse-scale equations are required. Some of the conditions have a straightforward justification, while others are dictated by simplicity and ease of implementation.

Coarse-scale conditions

(i) Time derivatives of the fine-scales are neglected. This *quasi-static* approximation is equivalent to assuming that the fine scales adjust instantaneously to complement the coarse scales. Some authors [14] have been arguing in favor of tracking in time the subgrid-scale component in the solution. However, this would involve the additional computational cost of storing and integrating in time the fine-scale component of the state variables.

(ii) For smooth flows, one can expect that the spaces $\mathcal{S}_\gamma, \mathcal{S}_\kappa$ are composed of smooth functions (in particular, *continuous* functions). Recalling that we have already defined the discrete spaces $\mathcal{S}^h_\gamma, \mathcal{S}^h_\kappa$ as spaces of continuous functions, we can conclude that in the case of smooth flow, also $\mathcal{S}'_\gamma, \mathcal{S}'_\kappa$ are constituted of continuous functions. The condition

$$\int_{\tilde{\mathcal{E}}} \psi^h \, [\![\boldsymbol{v}']\!] \, \mathrm{d}\tilde{\mathcal{E}} = 0 \tag{40}$$

represents a weak enforcement of the continuity of $\boldsymbol{v}'$ across element interfaces. Although in many instances not explicitly stated, this last condition is often implicitly invoked in SUPG stabilized formulation for compressible flows [17, 18, 20–23, 25–27].

(iii) Analogously, the condition

$$\int_{\partial\Omega} \psi^h \boldsymbol{v}' \cdot \boldsymbol{n} \, \mathrm{d}(\partial\Omega) = 0 \tag{41}$$

is weakly enforcing a vanishing fine-scale solution at the boundary of the domain Ω, where boundary conditions apply. This is again a fairly standard hypothesis in variational multiscale formulations [20, 21, 27].

With the previous conditions, (36) and (39) reduce to:

$$\int_\Omega \boldsymbol{\psi}^h \cdot (\rho\, \dot{\boldsymbol{v}}^h) \, \mathrm{d}\Omega - \int_\Omega (\nabla_x \cdot \boldsymbol{\psi}^h)(p^h + p') \, \mathrm{d}\Omega = 0 \,, \tag{42}$$

$$\int_\Omega \psi^h \left(\dot{p}^h + \rho\, c_s^2\, (\nabla_x \cdot \boldsymbol{v}^h)\right) \mathrm{d}\Omega - \int_\Omega \nabla_x \psi^h \cdot \left(\rho\, c_s^2\, \boldsymbol{v}'\right) = 0 \,. \tag{43}$$

The variational multiscale approach now requires to test the momentum and energy equations on the fine-scale spaces, that is,

$$\int_\Omega \boldsymbol{\psi}' \cdot (\rho \dot{\boldsymbol{v}}') \, \mathrm{d}\Omega - \int_\Omega (\nabla_x \cdot \boldsymbol{\psi}') p' \, \mathrm{d}\Omega = -\langle \mathsf{Res}^h_v, \boldsymbol{\psi}' \rangle \,, \tag{44}$$

$$\int_\Omega \psi' \left(\dot{p}' + \psi'\, \rho\, c_s^2\, (\nabla_x \cdot \boldsymbol{v}')\right) \mathrm{d}\Omega = -\langle \mathsf{Res}^h_\epsilon, \psi' \rangle \,, \tag{45}$$

where Res^h_v and Res^h_p are operators belonging to the dual spaces $(\mathcal{S}'_\kappa)^*$ and $(\mathcal{S}'_\gamma)^*$, the spaces of continuous linear functionals over $\mathcal{S}'_\kappa$ and $\mathcal{S}'_\gamma$, respectively. Recalling that, by definition, the test functions vanish where pure Dirichlet boundary conditions are applied, and that the discrete test and trial spaces are constituted of continuous functions (so that inter-element jumps vanish) the residual operators have the expressions:

$$\begin{aligned}\langle \mathsf{Res}^h_v, \boldsymbol{w} \rangle &= \int_\Omega \boldsymbol{w} \cdot (\rho^h \dot{\boldsymbol{v}}^h) \, \mathrm{d}\Omega - \int_\Omega (\nabla_x \cdot \boldsymbol{w}) p^h \, \mathrm{d}\Omega \\ &= \int_\Omega \boldsymbol{w} \cdot \left(\rho^h \dot{\boldsymbol{v}}^h + \nabla_x p^h\right) \mathrm{d}\Omega \,,\end{aligned} \tag{46}$$

$$\langle \mathsf{Res}^h_\epsilon, w \rangle = \int_\Omega w \left(\dot{p}^h + \rho\, c_s^2\, (\nabla_x \cdot \boldsymbol{v}^h)\right) \mathrm{d}\Omega \,. \tag{47}$$

Assuming (as usually reasonable) that w belongs to the space $L^2(\Omega)$ of square integrable functions, the Riesz Representation Theorem [6, 55] allows to identify

$$\mathsf{Res}^h_v = \rho\, \dot{\boldsymbol{v}}^h + \nabla_x p^h \,, \tag{48}$$

$$\mathsf{Res}^h_p = \dot{p}^h + \rho\, c_s^2\, (\nabla_x \cdot \boldsymbol{v}^h) \,, \tag{49}$$

where Res^h_v and Res^h_ϵ are now considered as elements of $L^2(\Omega)$. Ideally, one would like to solve exactly the fine-scale equations, but, in practice, this is rarely possible and, for the purpose of stabilization, *unnecessary*. In fact, simple approximated *ansatz* based on the scaling of the residual are sufficient to provide the needed stabilization mechanisms.

Fine-scale representation conditions

(iv) Probably the simplest possibility is to assume that

$$\boldsymbol{v}' = -\tau \frac{1}{\rho} \mathsf{Res}^h_v \,, \tag{50}$$

$$p' = -\tau\, \mathsf{Res}^h_p \,, \tag{51}$$

where τ is an appropriate parameter with the dimension of time. This amounts to postulate that the dynamics of the fine scale decouple, as the fine-scale velocity $\boldsymbol{v}'$ is assumed to depend only on the momentum equation residual Res^h_v, and the fine-scale pressure p' only on the pressure equation residual Res^h_p. The factor $1/\rho$ in front of Res^h_v is needed for a correct dimensional scaling of $\boldsymbol{v}'$.

(v) Using criteria similar to [43, 44, 46], the stabilization parameter τ can be defined as

$$\tau = c_\tau \frac{\Delta t}{2} \,. \tag{52}$$

In practice, τ represents the average effect of the Green's function associated with the fine-scale equations [7, 20, 21, 27]. For the purpose of constructing stabilization mechanisms, it is not necessary to have a very accurate approximation of the Green's function, and a correct scaling is sufficient. Consequently, there is some freedom in defining the constant c_τ. The choice $c_\tau = 2$ (for which $\tau = \Delta t$) seemed to give the best results in the computations in

[48], where a second-order predictor/multi-corrector time integrator was used. These findings where confirmed by the von Neumann analysis of stability for such algorithm [47], which reveals that, for $c_\tau = 2$ and three iterations of the predictor/corrector, the dispersion error is particularly small over the entire spectrum of discrete wave numbers. However, values in the range $[1/2, 3]$ also lead to robust and accurate solutions in the nonlinear case, proving that a sharp estimate of c_τ is not required. With different time-stepping procedures, alternative choices may be superior. For more details on this subject, the reader can refer to [47, 48].

Remark5. Only one definition of τ is used for both the pressure and velocity equations, governing the propagation of acoustic waves. Because pressure and velocity disturbances are always tightly coupled, using a different definition of τ for the momentum and pressure equations may have potentially negative effects on the dissipation and dispersion error characteristics of the stabilized algorithm [47].

Remark6. Similar results would have been obtained if the standard SUPG methodology for systems of equations were used in place of the multiscale analysis (see [13, 43, 44]). In fact, it is possible to rewrite the system of equations (30)–(31) as

$$\boldsymbol{A}_0 \dot{\boldsymbol{Y}} + \boldsymbol{A}_i \, \boldsymbol{Y}_{,x_i} = \boldsymbol{0} \, , \tag{53}$$

where $\boldsymbol{Y} = [\boldsymbol{v}^T, p]^T$, and

$$\boldsymbol{A}_0 = \begin{bmatrix} \rho \boldsymbol{I}_{3\times3} & \boldsymbol{0}_{3\times1} \\ \boldsymbol{0}_{1\times3} & 1 \end{bmatrix} , \tag{54}$$

$$\boldsymbol{A}_i = \begin{bmatrix} 0 & 0 & 0 & \delta_{1i} \\ 0 & 0 & 0 & \delta_{2i} \\ 0 & 0 & 0 & \delta_{3i} \\ \rho\, c_s^2 \delta_{1i} & \rho\, c_s^2 \delta_{2i} & \rho\, c_s^2 \delta_{3i} & 0 \end{bmatrix} , \tag{55}$$

with δ_{ij} the Kronecker tensor ($\delta_{ij} = 1$ if $i = j$, $\delta_{ij} = 0$ otherwise). The stabilization proposed in [13, 43, 44] follows a methodology similar to [17, 18, 22, 23, 25, 26] and yields:

$$\boldsymbol{Y}' = -\boldsymbol{\tau}(\boldsymbol{A}_0 \dot{\boldsymbol{Y}} + \boldsymbol{A}_i \, \boldsymbol{Y}_{,x_i}) = -\tau(\dot{\boldsymbol{Y}} + \boldsymbol{A}_0^{-1} \boldsymbol{A}_i \, \boldsymbol{Y}_{,x_i}) \, , \tag{56}$$

where $\boldsymbol{\tau} = \tau \boldsymbol{A}_0^{-1}$, so that

$$\dot{\boldsymbol{Y}} + \boldsymbol{A}_0^{-1} \boldsymbol{A}_i \, \boldsymbol{Y}_{,x_i} = \begin{bmatrix} \frac{1}{\rho} \mathsf{Res}_v^h \\ \mathsf{Res}_p^h \end{bmatrix} . \tag{57}$$

The fundamental reason why these derivations match the previously developed multiscale analysis is due to the fact that $\boldsymbol{\tau}$ has been chosen as a diagonal matrix. The precise definition of $\boldsymbol{\tau}$ is somewhat arbitrary, and many different approaches to its design have been proposed [13, 17, 18, 22, 23, 25, 26, 28, 31, 43, 44, 51, 52]. Had not $\boldsymbol{\tau}$ been diagonal, a fully coupled residual ansatz for $\boldsymbol{Y}'$ would have been obtained. This aspect is a consequence of the connection between $\boldsymbol{\tau}$ and the Green's function for the fine-scale equations [20, 21, 27].

Remark7. In the discussion to follow on the nonlinear case, it will be easy to appreciate that the variational multiscale approach and the more classical instantiations of the SUPG method for compressible flows may have some substantial differences in the overall structure of the stabilizing terms.

Remark8. In [13], a numerical stability analysis is presented for a SUPG-stabilized method applied to the system form of a general linear hyperbolic wave equation. Although the present work and the work in [13] have been developed over the years in complete independence and for different purposes, there are similarities in the form of the stabilizing operators, at least in the linear case. Most importantly, the detailed stability analysis in multiple dimensions included in [13] directly applies to the linearized acoustic system under investigation in the present article, and lays the theoretical foundations for a rigorous analysis of the proposed approach in the nonlinear case.

Summarizing, the classical stability analysis of SUPG methods for compressible flows [22–24, 29, 30, 50], and the recent work in [13] show that the proposed variational multiscale approach provides stability to formulations with equal-order interpolation for pressure and velocity. These results constitute a sound theoretical foundation for the nonlinear method which is described next. It is worthwhile at this point to present the overall stabilized variational form of the linearized acoustic problem:

$$\begin{aligned} 0 = & \int_\Omega \boldsymbol{\psi}^h \cdot \rho \dot{\boldsymbol{v}}^h \, \mathrm{d}\Omega - \int_\Omega (\nabla_x \cdot \boldsymbol{\psi}^h) p^h \, \mathrm{d}\Omega \\ & + \int_\Omega (\nabla_x \cdot \boldsymbol{\psi}^h) \, \tau \left(\dot{p}^h + \rho \, c_s^2 \, (\nabla_x \cdot \boldsymbol{v}^h) \right) \mathrm{d}\Omega \, , \end{aligned} \tag{58}$$

$$\begin{aligned} 0 = & \int_\Omega \psi^h \left(\dot{p}^h + \rho \, c_s^2 \, (\nabla_x \cdot \boldsymbol{v}^h) \right) \mathrm{d}\Omega \\ & + \int_\Omega \nabla_x \psi^h \cdot c_s^2 \, \tau \left(\rho \, \dot{\boldsymbol{v}}^h + \nabla_x p^h \right) \mathrm{d}\Omega \, . \end{aligned} \tag{59}$$

It is clear that the terms

$$\int_\Omega \tau \, c_s^2 \, (\nabla_x \cdot \boldsymbol{\psi}^h)(\nabla_x \cdot \boldsymbol{v}^h) \, \mathrm{d}\Omega \, , \tag{60}$$

$$\int_\Omega \tau \, c_s^2 \, \nabla_x \psi^h \cdot \nabla_x p^h \, \mathrm{d}\Omega \tag{61}$$

have a stabilizing effect on equations (58)–(59), since they are the weak forms of a divergence-type incomplete Laplacian of the velocity and a full Laplacian of the pressure, respectively. The stability analysis in [13] confirms such conjecture.

Remark9. It is interesting to observe the terms (60)–(61) scale with τc_s^2, which represents an acoustic-inspired kinematic viscosity. There are therefore some similarities between the stabilizing terms in (58)–(59) and the so-called linear artificial viscosity [5, 40, 54], used to control acoustic oscillations past shock fronts. There is however one major difference, since the linear artificial viscosity approach is not variationally consistent, and degrades the order of accuracy of the method to first order. In the case of the stabilized equations (58)–(59), the terms (60)–(61) do not degrade the original order of accuracy

of the method to first order, since they are complemented by time derivative terms to form complete, variationally consistent residuals (see also [47] for an analysis of formal order of accuracy).

Remark10. In the computations in [48], the artificial viscosities adopted to control oscillations at shock fronts do not contain the linear scaling [5]. Best results in numerical computations were obtained using only a quadratic viscosity of von Neumann-Richtmyer type [5, 53], indicating that the stabilizing term in (60)–(61) performed well in controlling numerical instabilities of acoustic nature.

4. Variational multiscale analysis of the nonlinear problem

4.1. Variational equations

As in the linear case, the first step in the development of a variational form for (5)–(8) is to define the *trial* spaces for the kinematic and thermodynamic variables, which characterize the *state* of the system. Let $\mathcal{S}_\kappa$ denote the space of admissible values for the kinematic variables (displacements, velocities, accelerations), and $\mathcal{S}_\gamma$ the space of admissible thermodynamic states (densities, pressures, internal energies). In addition, $\mathcal{V}_\kappa$ is the (test) space of variations (compatible with the boundary condition (9)) for the kinematic variables, and $\mathcal{V}_\gamma$ is the (test) space of variations for the thermodynamic variables. The complete variational problem reads:

Find $\rho, p, \epsilon \in \mathcal{S}_\gamma$, *and* $\boldsymbol{u}, \boldsymbol{v} \in \mathcal{S}_\kappa$, *such that,* $\forall \psi \in \mathcal{V}_\gamma$, $\forall \boldsymbol{\psi} \in \mathcal{V}_\kappa$,

$$0 = \int_{\Omega_0} \boldsymbol{\psi} \cdot (\dot{\boldsymbol{u}} - \boldsymbol{v}) \, \mathrm{d}\Omega_0 \,, \tag{62}$$

$$0 = \int_{\Omega_0} \psi \, (\rho_0 - \rho J) \, \mathrm{d}\Omega_0 \,, \tag{63}$$

$$0 = \int_{\Omega_0} \boldsymbol{\psi} \cdot (\rho_0 \dot{\boldsymbol{v}}) \, \mathrm{d}\Omega_0 - \int_{\Omega} (\nabla_x \cdot \boldsymbol{\psi}) \, p \, \mathrm{d}\Omega - \int_{\partial\Omega} \boldsymbol{\psi} \cdot \boldsymbol{t} \, \mathrm{d}(\partial\Omega) - \int_{\Omega} \boldsymbol{\psi} \cdot (\rho \boldsymbol{b}) \, \mathrm{d}\Omega \,, \tag{64}$$

$$0 = \int_{\Omega_0} \psi \, (\rho_0 \dot{\epsilon}) \, \mathrm{d}\Omega_0 + \int_{\Omega} \psi \, (p \nabla_x \cdot \boldsymbol{v} + \rho r) \, \mathrm{d}\Omega + \int_{\Omega} \nabla_x \psi \cdot \boldsymbol{q} \, \mathrm{d}\Omega \,, \tag{65}$$

where the identity $\rho_0 \, \mathrm{d}\Omega_0 = \rho \, \mathrm{d}\Omega$ has been used, stating that the mass of an infinitesimal particle $dm = \rho_0 \, \mathrm{d}\Omega_0$ does not change under the Lagrangian deformation map.

Remark11. In the current formulation, traction (i.e., *natural*) boundary conditions are imposed in (64) through the weak form, while the space $\mathcal{S}_\kappa$ incorporates the set of *essential* boundary conditions (9), that is, boundary conditions of kinematic (Dirichlet) type are imposed *strongly*.

4.2. Variational multiscale analysis and stabilization

It is important to observe that the following analysis applies in the case of smooth flows (smooth solutions), for which the fine scales are assumed small with respect to the coarse scales. In particular, in the case of nonlinear systems, the variational multiscale framework leverages a *local* linearization of the equations. As in the linear case, the first step consists in developing of a multiscale description of the solution. For the sake of simplicity, and without loss of generality, the heat source/sink r, the body force $\boldsymbol{b}$, and the thermal heat flux $\boldsymbol{q}$ are assumed absent. The exact solution for the state $\boldsymbol{Y} = [\boldsymbol{u}^T, \boldsymbol{v}^T, \rho, \epsilon, p]^T \in \mathcal{S}$ of the system is decomposed as $\boldsymbol{Y} = \boldsymbol{Y}^h + \boldsymbol{Y}'$, where $\boldsymbol{Y}^h \in \mathcal{S}^h$ is the *mesh*- or *coarse*-scale solution, and $\boldsymbol{Y}' \in \mathcal{S}'$ is the *subgrid*- or *fine*-scale solution, with $\mathcal{S} = \mathcal{S}^h \bigoplus \mathcal{S}'$. In the proposed spatial approximation, *all* variables (both kinematic and thermodynamic, including pressure, density and internal energy) are approximated by piece-wise linear, continuous functions (node-centered degrees-of-freedom). Consequently, the test-spaces for the equations consist of piece-wise linear, continuous functions. More precisely:

$$\mathcal{S}^h_\kappa = \Big\{ \boldsymbol{\psi}^h \in (C^0(\Omega))^{n_d} : \boldsymbol{\psi}^h\big|_{\Omega_e} \in (\mathcal{P}_1(\Omega_e))^{n_d}, \; \boldsymbol{\psi}^h = \boldsymbol{g}_{bc}(t) \text{ on } \partial\Omega^g \Big\} \,, \tag{66}$$

$$\mathcal{V}^h_\kappa = \Big\{ \boldsymbol{\psi}^h \in (C^0(\Omega))^{n_d} : \boldsymbol{\psi}^h\big|_{\Omega_e} \in (\mathcal{P}_1(\Omega_e))^{n_d}, \; \boldsymbol{\psi}^h = \boldsymbol{0} \text{ on } \partial\Omega^g \Big\} \,, \tag{67}$$

$$\mathcal{S}^h_\gamma = \Big\{ \psi^h \in C^0(\Omega) : \psi^h\big|_{\Omega_e} \in \mathcal{P}_1(\Omega_e), \Big\} \,, \tag{68}$$

$$\mathcal{V}^h_\gamma = \mathcal{S}^h_\gamma \,, \tag{69}$$

where $\boldsymbol{g}_{bc}(t)$ indicates the generalized essential (Dirichlet) boundary conditions, possibly dependent on time. For example, if $\mathcal{S}^h_\kappa$ is used to approximate displacements, then $\boldsymbol{g}_{bc} = \boldsymbol{u}_{bc}$. If instead $\mathcal{S}^h_\kappa$ is used to approximate velocities, then $\boldsymbol{g}_{bc}$ indicates a velocity at the boundary compatible with $\boldsymbol{u}_{bc}$. Hence:

$$\boldsymbol{u} = \boldsymbol{u}^h + \boldsymbol{u}' \,, \tag{70}$$

$$\boldsymbol{v} = \boldsymbol{v}^h + \boldsymbol{v}' \,, \tag{71}$$

$$\rho_0 = \rho_0^h + \rho_0' \,, \tag{72}$$

$$\rho = \rho^h + \rho' \,, \tag{73}$$

$$\epsilon = \epsilon^h + \epsilon' \,, \tag{74}$$

$$p = p^h + p' \,. \tag{75}$$

In the Lagrangian setting, the displacement and mass conservation equations (5)-(6) are associated with a standing entropy wave (with respect to the Lagrangian material coordinates) governing the motion of contact discontinuities. In this context, it is also important to observe that numerical schemes in Lagrangian coordinates, by construction, are capable of precisely capturing and tracking contact discontinuities without adding any numerical dissipation. Consequently, the incorporation of the equations (62)–(63) is not critical in the analysis, which can be restricted to equations (64) and (65). This simplified approach has the main advantage of producing a "minimalist stabilization", of easier numerical implementation. Namely, when

tested over the discrete spaces $\mathcal{V}^h_\kappa$ and $\mathcal{V}^h_\gamma$, (64) and (65) reduce to

$$0 = \int_{\Omega_0} \boldsymbol{\psi}^h \cdot (\rho_0^h + \rho_0')(\dot{\boldsymbol{v}}^h + \dot{\boldsymbol{v}}')\, \mathrm{d}\Omega_0 - \int_\Omega (\nabla_x \cdot \boldsymbol{\psi}^h)(p^h + p')\, \mathrm{d}\Omega \,, \tag{76}$$

$$0 = \int_{\Omega_0} \psi^h (\rho_0^h + \rho_0')(\dot{\epsilon}^h + \dot{\epsilon}')\, \mathrm{d}\Omega_0 + \int_\Omega \psi^h \left(\nabla_x \cdot (\boldsymbol{v}^h + \boldsymbol{v}')\right)(p^h + p')\, \mathrm{d}\Omega \,, \tag{77}$$

where, in order to simplify the analysis, homogenous Dirichlet boundary conditions are imposed for the velocity. The energy equation (77) can be rearranged, using integration by parts, as follows:

$$\begin{aligned} &\int_{\Omega_0} \psi^h (\rho_0^h + \rho_0')(\dot{\epsilon}^h + \dot{\epsilon}')\, \mathrm{d}\Omega_0 \\ &+ \int_\Omega \psi^h\, \nabla_x \cdot \boldsymbol{v}^h \left(p^h + p'\right) \mathrm{d}\Omega \\ &- \int_\Omega \nabla_x \psi^h \cdot \left((p^h + p')\boldsymbol{v}'\right) \mathrm{d}\Omega \\ &- \int_\Omega \psi^h \left(\nabla_x (p^h + p')\right) \cdot \boldsymbol{v}'\, \mathrm{d}\Omega \\ &+ \sum_{e=1}^{n_{el}} \int_{\partial\Omega_e} \psi^h \left(p^h + p'\right) \boldsymbol{v}' \cdot \boldsymbol{n}_e\, \mathrm{d}(\partial\Omega) = 0 \,. \end{aligned} \tag{78}$$

Recalling that ψ^h is continuous across element interfaces, the last term in (78) can be expressed as

$$\sum_{e=1}^{n_{el}} \int_{\partial\Omega_e} \psi^h \left(p^h + p'\right) \boldsymbol{v}' \cdot \boldsymbol{n}_e\, \mathrm{d}\Omega = \int_{\partial\Omega} \psi^h\, p\, \boldsymbol{v}' \cdot \boldsymbol{n}\, \mathrm{d}(\partial\Omega) + \int_{\tilde{\mathcal{E}}} \psi^h [\![p\boldsymbol{v}']\!]\, \mathrm{d}\tilde{\mathcal{E}} \,, \tag{79}$$

where, as in the linear case, $[\![\boldsymbol{w}]\!] = \boldsymbol{w}^- \cdot \boldsymbol{n}^- + \boldsymbol{w}^+ \cdot \boldsymbol{n}^+$ denotes the jump operator applied to $\boldsymbol{w}$, and $\tilde{\mathcal{E}}$ denotes the set of interior element interfaces. Then (78) becomes

$$\begin{aligned} &\int_{\Omega_0} \psi^h (\rho_0^h + \rho_0')(\dot{\epsilon}^h + \dot{\epsilon}')\, \mathrm{d}\Omega_0 \\ &+ \int_\Omega \psi^h\, \nabla_x \cdot \boldsymbol{v}^h \left(p^h + p'\right) \mathrm{d}\Omega \\ &- \int_\Omega \nabla_x \psi^h \cdot \left((p^h + p')\boldsymbol{v}'\right) \mathrm{d}\Omega \\ &- \int_\Omega \psi^h \left(\nabla_x (p^h + p')\right) \cdot \boldsymbol{v}'\, \mathrm{d}\Omega \\ &+ \int_{\partial\Omega} \psi^h\, p^h \boldsymbol{v}' \cdot \boldsymbol{n}\, \mathrm{d}(\partial\Omega) + \int_{\tilde{\mathcal{E}}} \psi^h [\![p^h \boldsymbol{v}']\!]\, \mathrm{d}\tilde{\mathcal{E}} = 0 \,. \end{aligned} \tag{80}$$

From now on, we will focus on the variational forms (76) and (80). Analogous projections of (76) and (80) onto the fine scale test spaces $\mathcal{V}'_\kappa$ and $\mathcal{V}'_\gamma$ can be considered, to generate the fine-scale problems. *No approximation* has been made so far, and the initial geometry of the computational grid, as well as the displacement field are assumed to be known *exactly*. In order to obtain a treatable problem, a number of conditions has to be enforced on the terms in the coarse-scale equations. As in the linear case, some of these conditions are straightforward, others are dictated by simplicity and ease of implementation.

Coarse-scale conditions

(i) Fine-scale terms are considered *small* with respect to coarse-scale terms. Therefore, if necessary, products of fine-scale terms can be neglected, being higher-order corrections. This is, essentially, a statement of local linearization of the variational problem under consideration.

(ii) Fine-scale components of the displacements $\boldsymbol{u}'$ (i.e., fine-scale node positions and mesh geometry) are considered negligible, with the purpose of a simpler implementation. Although not pursued here, there is a possibility to quantify these fine-scale contributions.

(iii) ρ_0' is considered negligible, since ρ_0 is a *datum* of the problem.

(iv) As in the linear case, time derivatives of the fine-scales are neglected, in favor of a quasi-static approximation.

(v) In order to preserve global conservation properties, we enforce as a design condition that the last three integral terms in (80) vanish. Let us review each of these conditions:

$$\int_\Omega \psi^h \left(\nabla_x (p^h + p')\right) \cdot \boldsymbol{v}'\, \mathrm{d}\Omega = 0 \tag{81}$$

enforces that the projection onto the test function space of the inner product between the pressure gradient and fine-scale viscosity vanishes. An equivalent interpretation is that, in a weak sense, the fine-scale component of the velocity does not produce any internal work. This condition can also be understood as the constraint on $\boldsymbol{v}'$ to be a zero-energy, hourglass mode [3, 5]. The condition

$$\int_{\partial\Omega} \psi^h\, p^h \boldsymbol{v}' \cdot \boldsymbol{n}\, \mathrm{d}(\partial\Omega) = 0 \tag{82}$$

weakly enforces that the fine-scale velocity does not produce any work at the boundary $\partial\Omega$ of the domain. This condition is equivalent to imposing that the fine-scale velocity vanishes at the boundary $\partial\Omega$, and, as already mentioned in Section 3.2, is a standard (often implicit) hypothesis in variational multiscale formulations [20, 21, 27]. Finally, the condition

$$\int_{\tilde{\mathcal{E}}} \psi^h [\![p^h \boldsymbol{v}']\!]\, \mathrm{d}\tilde{\mathcal{E}} = 0 \tag{83}$$

weakly enforces that the surface work $p^h \boldsymbol{v}' \cdot \boldsymbol{n}$, produced by the interaction of the fine-scale velocity and coarse-scale pressure, is continuous across element interfaces. In the case of a smooth $\boldsymbol{v}$, since p^h and $\boldsymbol{v}^h$ are continuous, this condition can also be justified by observing that $\boldsymbol{v}' = \boldsymbol{v} - \boldsymbol{v}^h$ must also be continuous. Notice that, although often not explicitly stated, (83) is implicitly invoked in most SUPG stabilized formulations for compressible flows.

With the previous conditions, (76) and (78) reduce to:

$$\int_{\Omega_0} \boldsymbol{\psi}^h \cdot (\rho_0^h \dot{\boldsymbol{v}}^h)\, \mathrm{d}\Omega_0 - \int_{\Omega} \nabla_x \cdot \boldsymbol{\psi}^h (p^h + p')\, \mathrm{d}\Omega = 0 \,, \tag{84}$$

$$\int_{\Omega_0} \psi^h (\rho_0^h \dot{\epsilon}^h)\, \mathrm{d}\Omega_0 + \int_{\Omega} \psi^h\, \nabla_x \cdot \boldsymbol{v}^h (p^h + p')\, \mathrm{d}\Omega - \int_{\Omega} \nabla_x \psi^h \cdot \left(p^h \boldsymbol{v}'\right) \mathrm{d}\Omega = 0 \,. \tag{85}$$

Remark12. Equations (84)–(85) present striking similarities with equations (42)–(43), once the integrals of the time derivatives are pushed forward to the current configuration:

$$\int_{\Omega} \boldsymbol{\psi}^h \cdot (\rho^h \dot{\boldsymbol{v}}^h)\, \mathrm{d}\Omega - \int_{\Omega} \nabla_x \cdot \boldsymbol{\psi}^h (p^h + p')\, \mathrm{d}\Omega = 0 \,, \tag{86}$$

$$\int_{\Omega} \psi^h \left(\rho^h \dot{\epsilon}^h + p^h\, \nabla_x \cdot \boldsymbol{v}^h\right) \mathrm{d}\Omega + \int_{\Omega} \psi^h p'\, \nabla_x \cdot \boldsymbol{v}^h\, \mathrm{d}\Omega - \int_{\Omega} \nabla_x \psi^h \cdot \left(p^h \boldsymbol{v}'\right) \mathrm{d}\Omega = 0 \,, \tag{87}$$

where, in particular,

$$\rho^h \dot{\epsilon}^h + p^h\, \nabla_x \cdot \boldsymbol{v}^h = \rho^h\, \partial_\epsilon p^h \big|_\rho^h \left(\dot{p}^h + \rho^h\, (c_s^h)^2\, (\nabla_x \cdot \boldsymbol{v}^h)\right) \,. \tag{88}$$

Therefore, the variational multiscale stabilization of the nonlinear case retains part of the structure of the linearized case. This observation is important in designing appropriate approximations to p' and $\boldsymbol{v}'$.

Remark13. The term

$$\int_{\Omega} \psi^h\, p'\, \nabla_x \cdot \boldsymbol{v}^h\, \mathrm{d}\Omega \tag{89}$$

is not present in the linearized case, and is of fundamental importance in preserving global conservation of total energy in the nonlinear case. It is also important to notice that this term would not appear if a standard SUPG approach were applied. Details on the global conservation properties of the proposed stabilization approach are presented in Section 5.2.

The variational multiscale approach now requires to test the momentum and energy equations on the fine-scale spaces $\mathcal{V}'_\kappa$ and $\mathcal{V}'_\gamma$, that is,

$$\int_{\Omega_0} \boldsymbol{\psi}' \cdot (\rho_0^h + \rho_0')\dot{\boldsymbol{v}}'\, \mathrm{d}\Omega_0 + \int_{\Omega_0} \boldsymbol{\psi}' \cdot (\rho_0' \dot{\boldsymbol{v}}^h)\, \mathrm{d}\Omega_0 - \int_{\Omega} (\nabla_x \cdot \boldsymbol{\psi}') p'\, \mathrm{d}\Omega = -\langle \mathsf{Res}_v^h, \boldsymbol{\psi}' \rangle \,, \tag{90}$$

$$\int_{\Omega_0} \psi' (\rho_0^h + \rho_0')\dot{\epsilon}'\, \mathrm{d}\Omega_0 + \int_{\Omega_0} \psi' \rho_0' \dot{\epsilon}^h\, \mathrm{d}\Omega_0 + \int_{\Omega} \psi'\, (\nabla_x \cdot (\boldsymbol{v}^h + \boldsymbol{v}'))p'\, \mathrm{d}\Omega + \int_{\Omega} \psi'\, (\nabla_x \cdot \boldsymbol{v}')p^h\, \mathrm{d}\Omega = -\langle \mathsf{Res}_\epsilon^h, \psi' \rangle \,, \tag{91}$$

where, for pure Dirichlet boundary conditions, $\langle \mathsf{Res}_v^h, \cdot \rangle \in (\mathcal{S}'_\kappa)^*$ and $\langle \mathsf{Res}_\epsilon^h, \cdot \rangle \in (\mathcal{S}'_\gamma)^*$ are defined by pushing forward to the current configuration and integrating by parts:

$$\langle \mathsf{Res}_v^h, \boldsymbol{w} \rangle = \int_{\Omega} \boldsymbol{w} \cdot \left(\rho^h \dot{\boldsymbol{v}}^h + \nabla_x p^h\right) \mathrm{d}\Omega \,, \tag{92}$$

$$\langle \mathsf{Res}_\epsilon^h, w \rangle = \int_{\Omega} w \left(\rho^h \dot{\epsilon}^h + (\nabla_x \cdot \boldsymbol{v}^h) p^h\right) \mathrm{d}\Omega \,. \tag{93}$$

As in the linear case, by means of the Riesz Representation Theorem, it is possible to identify the residual operators with the following members of the space $L^2(\Omega)$

$$\mathsf{Res}_v^h = \rho^h \dot{\boldsymbol{v}}^h + \nabla_x p^h \,, \tag{94}$$

$$\mathsf{Res}_\epsilon^h = \rho^h \dot{\epsilon}^h + (\nabla_x \cdot \boldsymbol{v}^h) p^h \,. \tag{95}$$

We now need to make further assumptions about the subgrid dynamics, to obtain a treatable fine-scale problem. The fundamental idea is to explore a simple solution *ansatz*, inspired by the results already obtained in the linear wave propagation case.

Fine-scale conditions

(vi) Recalling the structure of the momentum equation (25), we can assume the following structure for the fine-scale velocity:

$$\boldsymbol{v}' = -\tau \rho^h \frac{(c_s^h)^2}{p^h} \left.\frac{\partial \epsilon}{\partial p}\right|_\rho^h \mathsf{Res}_v^h \,, \tag{96}$$

where τ is defined as in (52). This produces the stabilizing term

$$p^h \boldsymbol{v}' = -\rho^h \left.\frac{\partial \epsilon}{\partial p}\right|_\rho^h \tau (c_s^h)^2\, \nabla_x \psi^h \cdot \mathsf{Res}_v^h \,. \tag{97}$$

(vii) Recalling the structure of the energy equation (26), we have that $\mathsf{Res}_\epsilon^h = \rho^h\, \partial_p \epsilon \big|_\rho^h \mathsf{Res}_p^h$, with

$$\mathsf{Res}_p^h = \dot{p}^h + \rho^h (c_s^h)^2\, \nabla_x \cdot \boldsymbol{v}^h \,. \tag{98}$$

It was shown in [46] that the expression for Res_p^h can also be derived by considering isentropic processes in perfect materials (materials free from internal dissipation mechanisms). It was also shown in [45, 46] that Res_p^h measures the *production* of entropy due to the numerical discretization. In regions of smooth flow, Res_p^h should vanish, but because of numerical instabilities, *numerical entropy* can be generated. At this point, it becomes natural to use the pressure residual to build an approximation to the fine-scale pressure as follows:

$$p' = -\tau\, \mathsf{Res}_p^h \,. \tag{99}$$

It was shown in [46] that the same approximation can be obtained by taking the difference $p' = p - p^h$ and linearizing the equation of state $p = \hat{p}(\rho, \epsilon)$ about p^h.

(viii) Because the system of equations at hand has the structure of a non-linear wave equation, it makes sense to use the same parameter τ in both the momentum and energy equations (see also [47] for more details on this interpretation from the point view of the von Neumann analysis of stability).

Remark14. In [46], the variational multiscale approach was used to stabilize formulations with piece-wise constant thermodynamic variables, enriching the discrete pressure by a fine-scale pressure defined as in (99). In the present approach, we also add the contribution of the fine-scale velocity $\boldsymbol{v}'$ to stabilize the energy equation.

Remark15. By definition, the terms $\boldsymbol{v}'$ and p' vanish at pure contact discontinuities, where the pressure and velocity are constant in space and time, and perfectly matched (equal) across the contact interface. Therefore, interpreting the term $p^h\boldsymbol{v}'$ as a heat flux term would be *utterly incorrect*. This term, instead, represents the work produced by the interaction between the fine-scale velocity and the coarse-scale pressure.

Remark16. When shock waves are present in the material, the analysis just presented does not apply. From a physical point of view, a shock wave is an infinitely thin layer in which the flow does not behave as a perfect material, due to internal dissipation mechanisms. At the numerical level, these irreversible mechanisms are introduced by shock-capturing operators in the form of artificial viscosities, which smear the discontinuity over a few cells of the computational grid.

It is now interesting to summarize the overall stabilized formulation obtained. Namely, (84)–(85) become:

$$\int_{\Omega_0} \boldsymbol{\psi}^h \cdot (\rho_0^h \dot{\boldsymbol{v}}^h)\, \mathrm{d}\Omega_0 - \int_\Omega \nabla_x \cdot \boldsymbol{\psi}^h \; p^h \; \mathrm{d}\Omega + \int_\Omega \nabla_x \cdot \boldsymbol{\psi}^h \; \tau \; \left(\dot{p}^h + \rho^h (c_s^h)^2 \; \nabla_x \cdot \boldsymbol{v}^h\right) \mathrm{d}\Omega = 0 \,, \tag{100}$$

$$\int_{\Omega_0} \psi^h (\rho_0^h \dot{\epsilon}^h)\, \mathrm{d}\Omega_0 + \int_\Omega \psi^h \; \nabla_x \cdot \boldsymbol{v}^h \; p^h \; \mathrm{d}\Omega + \int_\Omega \rho^h \left.\frac{\partial \epsilon}{\partial p}\right|_\rho^h \tau (c_s^h)^2 \; \nabla_x \psi^h \cdot \left(\rho^h \dot{\boldsymbol{v}}^h + \nabla_x p^h\right) \mathrm{d}\Omega + \int_\Omega \psi^h \; \nabla_x \cdot \boldsymbol{v}^h \; \tau \left(\dot{p}^h + \rho^h (c_s^h)^2 \; \nabla_x \cdot \boldsymbol{v}^h\right) \mathrm{d}\Omega = 0 \,. \tag{101}$$

Pushing forward some of the integrals to the current configuration, recalling $\mathsf{Res}_\epsilon^h = \rho^h \; \partial_p \epsilon\big|_\rho^h \mathsf{Res}_p^h$, and collecting terms yields:

$$0 = \int_\Omega \boldsymbol{\psi}^h \cdot (\rho^h \dot{\boldsymbol{v}}^h)\, \mathrm{d}\Omega - \int_\Omega \nabla_x \cdot \boldsymbol{\psi}^h \; p^h \; \mathrm{d}\Omega + \int_\Omega \nabla_x \cdot \boldsymbol{\psi}^h \; \tau \; \left(\dot{p}^h + \rho^h (c_s^h)^2 \; \nabla_x \cdot \boldsymbol{v}^h\right) \mathrm{d}\Omega \,, \tag{102}$$

$$0 = \int_\Omega \rho^h \left.\frac{\partial \epsilon}{\partial p}\right|_\rho^h \left(\psi^h \left(\dot{p}^h + \rho^h (c_s^h)^2 \; \nabla_x \cdot \boldsymbol{v}^h\right)\right) \mathrm{d}\Omega + \int_\Omega \rho^h \left.\frac{\partial \epsilon}{\partial p}\right|_\rho^h \left(\tau (c_s^h)^2 \; \nabla_x \psi^h \cdot \left(\rho^h \dot{\boldsymbol{v}}^h + \nabla_x p^h\right)\right) \mathrm{d}\Omega + \int_\Omega \psi^h \; \nabla_x \cdot \boldsymbol{v}^h \; \tau \left(\dot{p}^h + \rho^h (c_s^h)^2 \; \nabla_x \cdot \boldsymbol{v}^h\right) \mathrm{d}\Omega \,. \tag{103}$$

It is easy to appreciate that (102) is an almost identical (non-linear) statement of (58). The first two terms in equation (103) are almost identical to the terms in (59), with the exception that they are scaled by $\rho^h \; \partial_p \epsilon\big|_\rho^h$. As already mentioned, the last term in equation (103) is not present in (59), and is important in ensuring conservation of total energy of the overall formulation.

Remark17. Recalling that for an ideal gas

$$\rho^h \; \partial_p \epsilon\big|_\rho^h = 1/(\gamma - 1) \,, \tag{104}$$

the connection between (103) and its linear counterpart (59) is even more stringent.

Remark18. Stabilization is provided by the term

$$\int_\Omega \tau \; (c_s^h)^2 \rho^h \left(\nabla_x \cdot \boldsymbol{\psi}^h\right) \left(\; \nabla_x \cdot \boldsymbol{v}^h\right) \mathrm{d}\Omega \,, \tag{105}$$

$$\tag{106}$$

in the momentum equation (102), and by the terms

$$\int_\Omega \tau (c_s^h)^2 \; \rho^h \left.\frac{\partial \epsilon}{\partial p}\right|_\rho^h \left(\nabla_x \psi^h \cdot \nabla_x p^h\right) \mathrm{d}\Omega \,, \tag{107}$$

$$\int_\Omega \tau (c_s^h)^2 \; \psi^h \; \rho^h \left(\nabla_x \cdot \boldsymbol{v}^h\right)^2 \mathrm{d}\Omega \,, \tag{108}$$

in the energy equation (103). As in the linear wave propagation case, these stabilizing terms are scaled by the acoustic-type kinematic viscosity $\tau (c_s^h)^2$. Analogous to the linear case, since the stabilized formulation is residual-based and variationally consistent, it does not produce a degradation of the order of accuracy [47].

Remark19. As already mentioned at the end of Section 3.2, the value $c_\tau = 2$ (for which $\tau = \Delta t$) seems to give the best results in the computations in [48] for the nonlinear case. The von Neumann analysis of stability documented in [47] shows that this choice corresponds to very low dispersion error in the linearized version of the predictor/multi-corrector algorithm used in [48].

5. Invariance and conservation properties

5.1. Galilean Invariance

It is easy to verify that the proposed stabilization approach satisfies Galilean invariance properties, since the velocity appears in (100)–(101) always in differentiated form with respect to space or time. Galilean invariance properties were recognized as important in [41–43] in the specific case of Lagrangian and arbitrary Lagrangian-Eulerian (ALE) computations.

5.2. Global conservation

It is not very difficult to realize that the proposed algorithm conserves global mass (see [48] for the case of a specific time integrator), and momentum. In particular, global conservation of momentum in the ith direction is obtained by assuming homogenous Neumann (no traction) boundary conditions on the pressure, and testing the momentum equation (100) against $\boldsymbol{\psi}^h = \boldsymbol{e}_i$, the unit vector of the Cartesian basis in the ith direction. In this case, observing that $\nabla_x \cdot \boldsymbol{e}_i = 0$ we obtain:

$$\frac{\mathrm{d}}{\mathrm{d}t} \int_\Omega \boldsymbol{e}_i \cdot (\rho^h \boldsymbol{v}^h)\, \mathrm{d}\Omega = \int_{\Omega_0} \boldsymbol{e}_i \cdot (\rho_0^h \dot{\boldsymbol{v}}^h)\, \mathrm{d}\Omega_0 = 0 \,. \tag{109}$$

It is also not very difficult to verify that the system (100)–(101) satisfies conservation properties for the global total energy. In [48], this result is proved for a specific predictor/multi-corrector time integrator used in nonlinear computations. In this section, a general statement of broader applicability is proved. In the presentation of the key derivations, there is no need to have specific expressions for the fine scale terms. The stabilized equations of momentum and energy in the case of pure homogenous Neumann (traction) boundary conditions for the pressure are considered once more. Aside from the different function spaces on which these equations are defined, they look identical to equations (84)–(85), and are shown below for convenience:

$$\int_{\Omega_0} \boldsymbol{\psi}^h \cdot (\rho_0^h \dot{\boldsymbol{v}}^h)\, \mathrm{d}\Omega_0 - \int_\Omega \nabla_x \cdot \boldsymbol{\psi}^h (p^h + p')\, \mathrm{d}\Omega = 0 \,, \tag{110}$$

$$\int_{\Omega_0} \psi^h (\rho_0^h \dot{\epsilon}^h)\, \mathrm{d}\Omega_0 + \int_\Omega \psi^h\, \nabla_x \cdot \boldsymbol{v}^h (p^h + p')\, \mathrm{d}\Omega - \int_\Omega \nabla_x \psi^h \cdot \left(p^h \boldsymbol{v}'\right)\, \mathrm{d}\Omega = 0 \,. \tag{111}$$

Since homogeneous Neumann conditions are applied (no traction and traction work at the boundary), it is clear that $\boldsymbol{v}^h \in \mathcal{S}^h$ also belong to the test function space $\mathcal{V}^h$. Therefore, (110) can be tested against $\boldsymbol{\psi}^h = \boldsymbol{v}^h$, obtaining an equation for the evolution of the kinetic energy. For the same reason, it is also possible to choose $\psi^h = 1$ over the entire computational domain, and in this case $\nabla_x \psi^h = \boldsymbol{0}$. Using the push-forward to the current configuration and the identity $\rho_0\, \mathrm{d}\Omega_0 = \rho\, \mathrm{d}\Omega$, it is easy to derive:

$$\frac{\mathrm{d}}{\mathrm{d}t} \int_\Omega \frac{1}{2} \rho^h\, (\boldsymbol{v}^h \cdot \boldsymbol{v}^h)\, \mathrm{d}\Omega = \int_\Omega \nabla_x \cdot \boldsymbol{v}^h (p^h + p')\, \mathrm{d}\Omega \,, \tag{112}$$

$$\frac{\mathrm{d}}{\mathrm{d}t} \int_\Omega \rho^h\, \epsilon^h\, \mathrm{d}\Omega = -\int_\Omega \nabla_x \cdot \boldsymbol{v}^h (p^h + p')\, \mathrm{d}\Omega \,. \tag{113}$$

Summing equations (112)–(113), the right-hand sides cancel, yielding

$$\frac{\mathrm{d}}{\mathrm{d}t} \int_\Omega \rho^h \left(\frac{1}{2}\, (\boldsymbol{v}^h \cdot \boldsymbol{v}^h) + \epsilon^h \right) \mathrm{d}\Omega = 0 \,, \tag{114}$$

which is a statement of conservation of global total energy for the proposed stabilized approach.

Remark20. The presence of the term involving $\nabla_x \cdot \boldsymbol{v}^h p'$ in the energy equation (111) is crucial in obtaining the cancellation of terms which makes possible global conservation.

6. Summary

This work documents the development of a theoretical framework for updated Lagrangian stabilized formulations of Lagrangian shock hydrodynamics. The analysis apply to materials obeying a generalized caloric (e.g., Mie-Grüneisen) equation of state. The presentation of the main concepts has been performed first in the simpler linearized system of acoustic equations, and then generalized to the full nonlinear system of Lagrangian shock hydrodynamics equations. The proposed stabilization approach preserves global conservation and Galilean invariance properties in the nonlinear case. The extensive computations in [48] show the promise of the method, also in comparison with previous work done by the author and collaborators on the subject [43, 44]. The reader can also refer to [47], in which a von Neumann stability analysis of the method is performed for the specific time integrator adopted in the numerical computations in [48].

Acknowledgments

The author would like to acknowledge and thank for very valuable discussions Professor T. J. R. Hughes, at the University of Texas in Austin, Dr. M. Shashkov and Dr. L. Margolin at Los Alamos National Laboratory, Dr. J. Shadid, Dr. E. Love, Dr. W. Rider, Dr. A. Robinson, Dr. P. Bochev, and Dr. J. Carpenter at Sandia National Laboratories, Dr. B. Déspres and Dr. B. Rebourcet at Commissariat à l'Energie Atomique (CEA, France), Dr. P.-H. Maire at UMR-CELIA-CEA-University of Bordeaux, Dr. M. Ricchiuto at INRIA-Bordeaux, Prof. R. Abgrall at the University of Bordeaux, and Dr. Santiago Badia, at Universitat Politècnica de Catalunya (Barcelona). The author would also like to thank Dr. R. Summers and Dr. S. Collis at Sandia National Laboratories, for support and encouragement during the development of this research work.

References

[1] R. W. Anderson, N. S. Elliott, and R. B. Pember. An arbitrary Lagrangian-Eulerian method with adaptive mesh refinement for the solution of the Euler equations. *Journal of Computational Physics*, **199**(2):598–617, 2004.

[2] A. Barlow. A compatible finite element multi-material ALE hydrodynamics algorithm. *International Journal for Numerical Methods in Fluids*, **56**(8):953–964, 2008.

[3] T. Belytschko, W. K. Liu, and B. Moran. *Nonlinear Finite Elements for Continua and Structures*. J. Wiley & Sons, New York, 2000.

[4] D. J. Benson. A new two-dimensional flux-limited shock viscosity for impact calculations. *Computer Methods in Applied Mechanics and Engineering*, **93**:39–95, 1991.

[5] D. J. Benson. Computational methods in Lagrangian and Eulerian hydrocodes. *Computer Methods in Applied Mechanics and Engineering*, **99**:235–394, 1992.

[6] H. Brezis. *Analyse Fonctionnelle: Théorie et Applications*. Dunod, Paris, 1983.

[7] F. Brezzi, L. P. Franca, T. J. R. Hughes, and A. Russo. $b = \int g$. *Computer Methods in Applied Mechanics and Engineering*, **145**(3-4):329–339, 1997.

[8] J. C. Campbell and M. J. Shashkov. A compatible Lagrangian algorithm for unstructured grids. Technical report, LA-UR-00-3231, Los Alamos National Laboratory, 2000.

[9] J. C. Campbell and M. J. Shashkov. A tensor artificial viscosity using a mimetic finite difference algorithm. Technical report, LA-UR-00-2290, Los Alamos National Laboratory, 2000.

[10] J. C. Campbell and M. J. Shashkov. A tensor artificial viscosity using a mimetic finite difference algorithm. *Journal of Computational Physics*, **172**:739–765, 2001.

[11] E. J. Caramana and M. J. Shashkov. Elimination of artificial grid distortion and hourglass-type motions by means of Lagrangian subzonal masses and pressures. *Journal of Computational Physics*, **142**(2):521–561, 1998.

[12] E. J. Caramana, M. J. Shashkov, and P. P. Whalen. Formulations of artificial viscosity for multi-dimensional shock wave computations. *Journal of Computational Physics*, **144**:70–97, 1998.

[13] R. Codina. Finite element approximation of the hyperbolic wave equation in mixed form. *Computer Methods in Applied Mechanics and Engineering*, **197**(13-16):1305–1322, 2008.

[14] R. Codina, J. Principe, O. Guasch, and S. Badia. Time dependent subscales in the stabilized finite element approximation of incompressible flow problems. *Computer Methods in Applied Mechanics and Engineering*, **196**(21-24):2413–2430, 2007.

[15] B. Després and C. Mazeran. Symmetrization of Lagrangian gas dynamic in dimension two and multidimensional solvers. *Comptes Rendus Mecanique*, 331(7):475–480, 2003.

[16] B. Després and C. Mazeran. Lagrangian gas dynamics in two dimensions and Lagrangian systems. *Archives of Rational Mechanics and Analysis*, 178(3):327–372, 2005.

[17] G. Hauke and T. J. R. Hughes. A unified approach to compressible and incompressible flows. *Computer Methods in Applied Mechanics and Engineering*, **113**:389–396, 1994.

[18] G. Hauke and T. J. R. Hughes. A comparative study of different sets of variables for solving compressible and incompressible flows. *Computer Methods in Applied Mechanics and Engineering*, **153**:1–44, 1998.

[19] T. J. R. Hughes. *The Finite Element Method: Linear Static and Dynamic Finite Element Analysis*. Prentice-Hall, Englewood Cliffs, New Jersey, 1987. (Dover reprint, 2000).

[20] T. J. R. Hughes. Multiscale phenomena: Green's functions, the Dirichlet-to-Neumann formulation, subgrid-scale models, bubbles and the origin of stabilized methods. *Computer Methods in Applied Mechanics and Engineering*, **127**:387–401, 1995.

[21] T. J. R. Hughes, G.R. Feijóo, L. Mazzei, and J.-B. Quincy. The Variational Multiscale Method — a paradigm for computational mechanics. *Computer Methods in Applied Mechanics and Engineering*, **166**:3–24, 1998.

[22] T. J. R. Hughes, L. P. Franca, and G. M. Hulbert. A new finite element formulation for computational fluid dynamics: VIII. The Galerkin/least-squares method for advective-diffusive equations. *Computer Methods in Applied Mechanics and Engineering*, **73**:173–189, 1989.

[23] T. J. R. Hughes, L. P. Franca, and M. Mallet. A new finite element formulation for computational fluid dynamics: I. Symmetric forms of the compressible Euler and Navier-Stokes equations and the second law of thermodynamics. *Computer Methods in Applied Mechanics and Engineering*, **54**:223–234, 1986.

[24] T. J. R. Hughes, L. P. Franca, and M. Mallet. A new finite element formulation for computational fluid dynamics: VI. Convergence analysis of the generalized SUPG formulation for linear time-dependent multidimensional advective-diffusive systems. *Computer Methods in Applied Mechanics and Engineering*, **63**:97–112, 1987.

[25] T. J. R. Hughes and M. Mallet. A new finite element formulation for computational fluid dynamics: III. The generalized streamline operator for multidimensional advective-diffusive systems. *Computer Methods in Applied Mechanics and Engineering*, **58**:305–328, 1986.

[26] T. J. R. Hughes, M. Mallet, and A. Mizukami. A new finite element formulation for computational fluid dynamics: II. Beyond SUPG. *Computer Methods in Applied Mechanics and Engineering*, **54**:341–355, 1986.

[27] T. J. R. Hughes, G. Scovazzi, and Franca L.P. Multiscale and stabilized methods. In E. Stein, R. de Borst, and T. J. R. Hughes, editors, *Encyclopedia of Computational Mechanics*. John Wiley & Sons, 2004.

[28] T. J. R. Hughes and T. E. Tezduyar. Finite element methods for first-order hyperbolic systems with particular emphasis on the compressible Euler equations. *Computer Methods in Applied Mechanics and Engineering*, **45**:217–284, 1984.

[29] C. Johnson and A. Szepessy. On the convergence of a finite element method for a nonlinear hyperbolic conservation law. *Mathematics of Computation*, **49**:427–444, 1987.

[30] C. Johnson, A. Szepessy, and P. Hasnbo. On the convergence of shock-capturing streamline diffusion finite element methods for hyperbolic conservation laws. *Mathematics of Computation*, **54**:107–129, 1990.

[31] G. J. Le Beau, S. E. Ray, S. K. Aliabadi, and T. E. Tezduyar. SUPG finite element computation of compressible flows with the entropy and conservation variables formulations. *Computer Methods in Applied Mechanics and Engineering*, **195**:1621–1632, 2006.

[32] P.-H. Maire. A high-order cell-centered Lagrangian scheme for two-dimensional compressible fluid flows on unstructured meshes. accepted, J. Comput. Phys., doi:10.1016/j.jcp.2008.12.007, 2009.

[33] P.-H. Maire and J. Breil. A second-order cell-centered Lagrangian scheme for two-dimensional compressible flow problems. *International Journal for Numerical Methods in Fluids*, **56**:1417–1423, 2008.

[34] P.-H. Maire and B. Nkonga. Multi-scale Godunov-type method for cell-centered discrete Lagrangian hydrodynamics. to be pusblished in J. Comput. Phys. and available at http://hal.inria.fr/inria-00290717/fr/, 2008.

[35] L. G. Margolin. A centered artificial viscosity for cells with large aspect ratios. Technical report, UCRL-53882, Lawrence Livermore National Laboratory, 1988.

[36] L. G. Margolin and M. Shashkov. Second-order sign-preserving conservative interpolation (remapping) on general grids. *Journal of Computational Physics*, 184(1):266–298, 2003.

[37] L. G. Margolin and M. Shashkov. Remapping, recovery and repair on a staggered grid. *Computer Methods in Applied Mechanics and Engineering*, 193(39-41):4139–4155, 2004.

[38] L. G. Margolin and M. Shashkov. Finite volume methods and the equations of finite scale: A mimetic approach. *International Journal for Numerical Methods in Fluids*, 56(8):991–1002, 2008.

[39] R. Menikoff and B. J. Plohr. The Riemann problem for fluid flow of real materials. *Reviews of Modern Physics*, **61**(1):75–130, 1989.

[40] W. F. Noh. Errors for calculations of strong shocks using an artificial viscosity and an artificial heat flux. *Journal of Computational Physics*, **72**:78–120, 1987.

[41] G. Scovazzi. A discourse on Galilean invariance and SUPG-type stabilization. *Computer Methods in Applied Mechanics and Engineering*, **196**(4–6):1108–1132, 2007.

[42] G. Scovazzi. Galilean invariance and stabilized methods for compressible flows. *International Journal for Numerical Methods in Fluids*, **54**(6–8):757–778, 2007.

[43] G. Scovazzi. Stabilized shock hydrodynamics: II. Design and physical interpretation of the SUPG operator for Lagrangian computations. *Computer Methods in Applied Mechanics and Engineering*, **196**(4–6):966–978, 2007.

[44] G. Scovazzi, M. A. Christon, T. J. R. Hughes, and J. N. Shadid. Stabilized shock hydrodynamics: I. A Lagrangian method. *Computer Methods in Applied Mechanics and Engineering*, **196**(4–6):923–966, 2007.

[45] G. Scovazzi, E. Love, and M. J. Shashkov. A multi-scale Q1/P0 approach to Lagrangian shock hydrodynamics. Technical report, SAND2007-1423, Sandia National Laboratories, New Mexico, March 2007. Available at: `http://www.cs.sandia.gov/~gscovaz`.

[46] G. Scovazzi, E. Love, and M. J. Shashkov. A multi-scale Q1/P0 approach to Lagrangian shock hydrodynamics. *Computer Methods in Applied Mechanics and Engineering*, **197**(9–12):1056–1079, 2008.

[47] G. Scovazzi, W. J. Rider, E. Love, and J. N. Shadid. Stabilized shock hydrodynamics: V. Von Neumann stability analysis of a predictor/multi-corrector Lagrangian method. Computer Methods in Applied Mechanics and Engineering, 2009. Submitted.

[48] G. Scovazzi, J. N. Shadid, E. Love, and T. J. R. Hughes. Stabilized shock hydrodynamics: IV. Computations with a conservative updated Lagrangian method. Computer Methods in Applied Mechanics and Engineering, 2009. Submitted.

[49] J. C. Simo and T. J. R. Hughes. *Computational Inelasticity*. Springer, New York, 1998.

[50] A. Szepessy. Convergence of a shock-capturing streamline diffusion finite element method for a scalar conservation law in two space dimensions. *Mathematics of Computation*, **53**:527–545, 1989.

[51] T. E. Tezduyar and M. Senga. Stabilization and shock-capturing parameters in SUPG formulation of compressible flows. *Computer Methods in Applied Mechanics and Engineering*, **104**:397–422, 1993.

[52] T. E. Tezduyar, M. Senga, and D. Vicker. Computation of inviscid supersonic flows around cylinders and spheres with the SUPG formulation and YZβ shock-capturing. *Computational Mechanics*, **38**:469–481, 2006.
[53] J. von Neumann and R. D. Richtmyer. A method for the numerical computation of hydrodynamic shocks. *Journal of Applied Physics*, **21**:232–237, 1950.
[54] M. L. Wilkins. Use of artificial viscosity in multidimensional shock wave problems. *Journal of Computational Physics*, **36**:281–303, 1979.
[55] K. Yosida. *Functional Analysis*. Springer, New York, 1995.